

This article was downloaded by: [Korea University]

On: 07 October 2012, At: 23:10

Publisher: Taylor & Francis

Informa Ltd Registered in England and Wales Registered Number: 1072954

Registered office: Mortimer House, 37-41 Mortimer Street, London W1T 3JH, UK



## Journal of Adhesion Science and Technology

Publication details, including instructions for authors and subscription information:

<http://www.tandfonline.com/loi/tast20>

### Effect of curing temperature on the adhesion strength of polyamideimide/copper joints

J.H. Cho <sup>a</sup>, D.I. Kong <sup>b</sup>, C.E. Park <sup>c</sup> & M.Y. Jin <sup>d</sup>

<sup>a</sup> Polymer Research Institute, Department of Chemical Engineering, Pohang University of Science and Technology, Pohang 790-784, Korea

<sup>b</sup> Polymer Research Institute, Department of Chemical Engineering, Pohang University of Science and Technology, Pohang 790-784, Korea

<sup>c</sup> Polymer Research Institute, Department of Chemical Engineering, Pohang University of Science and Technology, Pohang 790-784, Korea

<sup>d</sup> Advanced Polymer Division, Korea Research Institute of Chemical Technology, Taejon 305-606, Korea

Version of record first published: 02 Apr 2012.

To cite this article: J.H. Cho, D.I. Kong, C.E. Park & M.Y. Jin (1998): Effect of curing temperature on the adhesion strength of polyamideimide/copper joints, Journal of Adhesion Science and Technology, 12:5, 507-521

To link to this article: <http://dx.doi.org/10.1163/156856198X00191>

PLEASE SCROLL DOWN FOR ARTICLE

Full terms and conditions of use: <http://www.tandfonline.com/page/terms-and-conditions>

This article may be used for research, teaching, and private study purposes. Any substantial or systematic reproduction, redistribution, reselling, loan, sub-licensing, systematic supply, or distribution in any form to anyone is expressly forbidden.

The publisher does not give any warranty express or implied or make any representation that the contents will be complete or accurate or up to date. The accuracy of any instructions, formulae, and drug doses should be independently verified with primary sources. The publisher shall not be liable for any loss, actions, claims, proceedings, demand, or costs or damages whatsoever or howsoever caused arising directly or indirectly in connection with or arising out of the use of this material.

## Effect of curing temperature on the adhesion strength of polyamideimide/copper joints

J. H. CHO<sup>1</sup>, D. I. KONG<sup>1</sup>, C. E. PARK<sup>1,\*</sup> and M. Y. JIN<sup>2</sup>

<sup>1</sup> *Polymer Research Institute, Department of Chemical Engineering, Pohang University of Science and Technology, Pohang 790-784, Korea*

<sup>2</sup> *Advanced Polymer Division, Korea Research Institute of Chemical Technology, Taejon 305-606, Korea*

Received in final form 20 December 1997

**Abstract**—The adhesion strength of polyamideimide (PAI)/copper joints was investigated as a function of the curing temperature and time. The adhesion strength decreased as the thermal stress increased with the increase of both curing temperature and time. The effects of copper oxide formed by thermal treatment and alkaline treatment on the adhesion strength of PAI/copper joints were examined. The adhesion strength decreased with thermally oxidized copper and increased with alkali-oxidized copper. The locus of failure of PAI/copper joints was also studied by scanning electron microscopy (SEM) and X-ray photoelectron spectroscopy (XPS). The locus of failure appears to be partially cohesive in both PAI and copper oxide.

**Keywords:** Polyamideimide (PAI); copper; adhesion strength; thermal stress; copper oxide.

### 1. INTRODUCTION

Polymer-coated copper wire, so-called enamel wire, is widely used in the electronics industry. Since a rolled enamel coil is used in electronic devices as an electronic-magnetic energy exchanger, considerable heat is generated and this heat can deteriorate the properties of polymeric coating materials, the adhesion strength between coating materials and copper, and the insulating capability of coating materials [1].

Polyamideimides (PAIs) used as coating materials have advantages of both polyamides and polyimides in their characteristics such as high chemical resistance, low dielectric constant, excellent mechanical and thermal properties, and good solvent resistance [2, 3]. Therefore, they are currently receiving considerable attention for their application in the aerospace, automotive, electronic, and related industries. Recently, since electronic devices of a smaller size, higher performance, and higher

---

\*To whom correspondence should be addressed. E-mail: cep@postech.ac.kr

reliability are required, high-temperature-resistant polymeric material such as polyimide and polyamideimide having good insulating property and a good adhesion strength to copper are needed [4–6]. In the case of a polymer–metal system, thermal stress is generated due to the thermal expansion coefficient mismatch. This thermal stress reduces the adhesion strength between the polymer and metal, and induces delamination at the interface and fracture of the polymer film, which can cause the malfunction of electronic devices [7, 8]. In order to prevent weakening of the adhesion strength, a flexible chain is introduced into the backbone of the polymer chain and a plasticizer is added to reduce the thermal stress at the interface. Also surface treatment of metals as well as coupling agents are used to improve the adhesion strength of polymer/metal joints [9–12].

It has also been reported that in polymer/copper joints, dense copper oxide formation can improve the adhesion strength [13, 14]. In this study, the adhesion strength of polyamideimide/copper joints was investigated and thermal stress was studied as a function of the curing temperature. The effects of copper oxide formed by thermal treatment and alkaline treatment on the adhesion strength were also examined.

## 2. EXPERIMENTAL

### 2.1. Materials

Polyamideimide (PAI) (Fig. 1) was supplied by Alsthom Chemical Co. (France). It was dissolved in a solvent mixture of *N*-methyl-2-pyrrolidone (NMP) and naphtha, and the solid content was 27.8 wt%. Copper coupons (thickness: 2 mm) were obtained from Poongsan Corp. (Angang, Korea).

### 2.2. Preparation of the peel test samples of PAI/copper joints

Copper coupons were immersed in chloroform (Junsei Chemical Co., Japan) for 20 min to remove organic materials, washed with distilled water, and then immersed in diluted sulfuric acid (5 wt%, Aldrich Chemical Co.) for 3 min to eliminate the natural copper oxide. The cleaned copper coupons were bar-coated with PAI solution and prebaked at 150°C for 60 min in a nitrogen atmosphere to form a

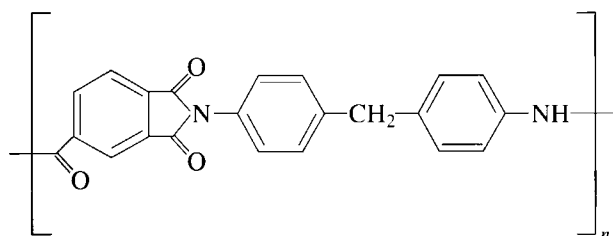


**Figure 1.** Structure of polyamideimide (PAI).

40  $\mu\text{m}$  thick PAI layer. The PAI was then cured at 200°C for 60 min and further cured at 250°C, 300°C, and 350°C. Four different samples of PAI/copper joints were prepared depending on the curing conditions as follows:

- PAI-200: 150°C for 60 min and 200°C for 60 min.
- PAI-250: 150°C for 60 min, 200°C for 60 min, and 250°C for 60 min.
- PAI-300: 150°C for 60 min, 200°C for 60 min, and 300°C for 60 min.
- PAI-350: 150°C for 60 min, 200°C for 60 min, and 350°C for 60 min.

### 2.3. Peel strength of PAI/copper joints

The adhesion strength of PAI/copper joints was measured by a 90° peel test at a peel rate of 10 mm/min using an Instron (Model 4206).

### 2.4. Fourier transform infrared (FT-IR) spectroscopy

Delaminated PAI films from PAI/copper joints were examined by using a FT-IR spectrometer from Mattson Instruments, Inc.

### 2.5. Thermal analysis

The glass transition temperature ( $T_g$ ) was measured using a differential scanning calorimeter (Perkin–Elmer DSC-7) at a heating rate of 20°C/min. Thermogravimetric analysis (TGA) of the four different samples (PAI-200, PAI-250, PAI-300, and PAI-350) was performed using Perkin–Elmer TGA-7 equipment at a scanning rate of 10°C/min in an air environment. The linear thermal expansion coefficient was determined using a thermo-mechanical analyzer (Seiko Instrument TMA 120CU). The storage modulus was measured between –50 and 300°C at a heating rate of 3°C/min and a frequency of 1 Hz in nitrogen atmosphere, using a dynamic mechanical thermal analyzer (Polymer Laboratories, Loughborough, UK).

### 2.6. Residual stress measurements

The curvature of copper coupons with and without a PAI film was measured using a homemade thin film stress analyzer, which was equipped with a He–Ne laser and a heat stage in a dry nitrogen atmosphere and controlled by a personal computer. In actual measurements, the variations of the angle  $\theta$  between the incident and the reflected laser light beams were monitored as in Fig. 2. The distance  $x$  between the two beams was 63.5 mm. Therefore, the curvature  $R$  of the copper coupon can be calculated from the angle and the distance as  $R = x/\theta$ . Then the residual stress ( $\sigma_r$ ) in the PAI film was calculated from the radii of curvature of the copper coupon measured before and after coating with a PAI film using the equation [15–18]:

$$\sigma_r = \frac{1}{6} \frac{E_s t_S^2}{1 - \nu_S} \left( \frac{1}{R_F} - \frac{1}{R_\infty} \right). \quad (1)$$

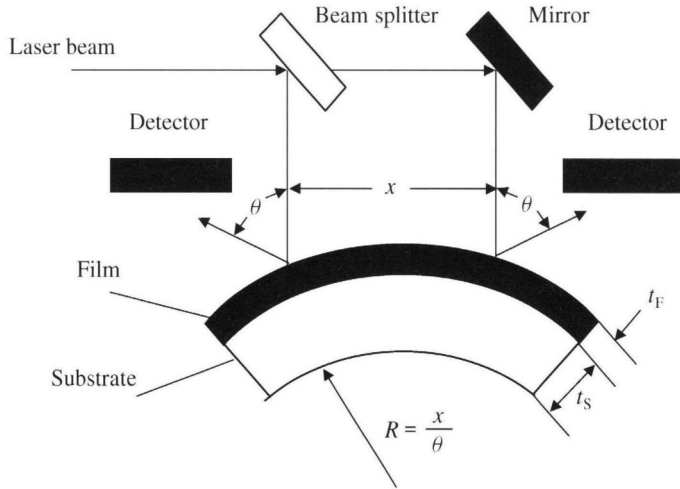


**Figure 2.** Schematic diagram of the He–Ne laser thin film stress analyzer.

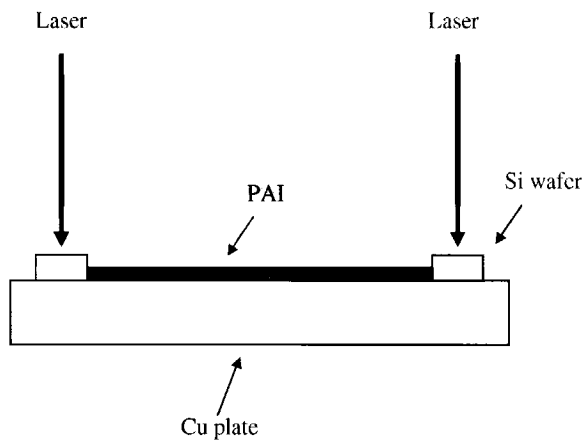


**Figure 3.** Schematic diagram of the residual stress measurement of PAI/copper joints.

Here, the subscripts F and S denote the PAI film and the copper substrate, respectively. The symbols  $E$ ,  $\nu$ , and  $t$  are Young's modulus, Poisson's ratio, and the thickness of each layer material, respectively.  $R_F$  and  $R_\infty$  are the radii of the Si wafer with and without a PAI film, respectively. Since the surface of the copper coupon is relatively rough and He–Ne laser light is scattered on the copper surface, rectangular silicon wafer pieces ( $1 \times 1$  cm) were attached, using pyromellitic dianhydride–oxydianiline (PMDA-ODA) polyimide as an adhesive, to the copper coupon where the He–Ne laser light was focused (Fig. 3). Then the PAI was spin-coated and prebaked at  $80^\circ\text{C}$ , and this process was repeated to make a  $75 \mu\text{m}$  thick PAI film. The variation of residual stress was investigated versus the curing temperature, where the temperature was raised at a rate of  $2^\circ\text{C}/\text{min}$ .

The residual stress ( $\sigma_r$ ) is the sum of intrinsic ( $\sigma_i$ ) and thermal stress ( $\sigma_t$ ), and the thermal stress can be expressed by the equation [19]:

$$\sigma_t = (\alpha_F - \alpha_S)(T_F - T) \frac{E_F}{1 - \nu_F}, \quad (2)$$

where  $\alpha$  is the thermal expansion coefficient,  $T_F$  is the final curing temperature ( $T_F = T_g$  if  $T_g \leq T_F$ ), and  $T$  is the stress measurement temperature.

### 2.7. Locus of failure

The locus of failure was investigated by using SEM using a Hitachi S-570 spectrometer and XPS using a Perkin–Elmer Phi-5400 spectrometer.

### 2.8. Formation of copper oxide

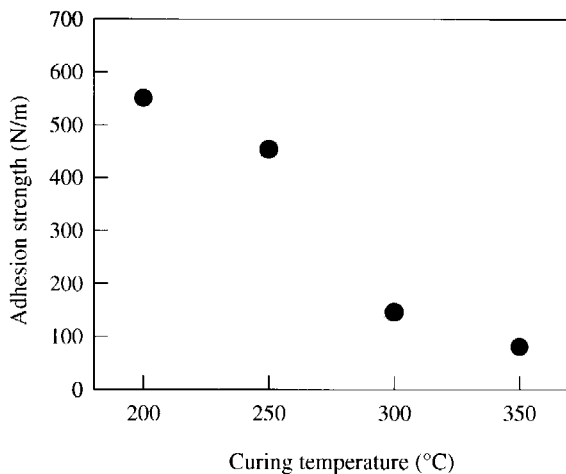
Before forming copper oxide, the copper surface was degreased with chloroform and then the natural oxide was removed by immersion in dilute sulfuric acid. Thermally formed copper oxide was produced by storing the copper coupons in a 150°C or 200°C oven for 2 h. Chemically formed copper oxide was created by treating the copper coupons with sodium chlorite and sodium hydroxide solution (NaClO<sub>2</sub> 37.5 g, NaOH 6 g, Na<sub>3</sub>PO<sub>4</sub> · 12H<sub>2</sub>O 25 g, and H<sub>2</sub>O 1000 g) at 85°C for 2 min [20]. This alkali-formed oxide was rinsed with distilled water and dried in a convection oven at 110°C for 30 min.

## 3. RESULTS AND DISCUSSION

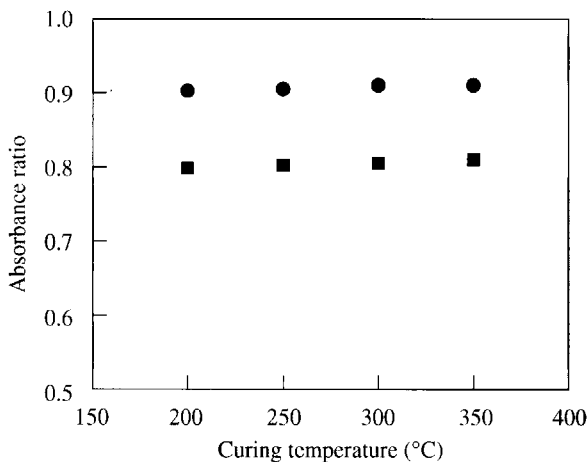
### 3.1. Adhesion strength of PAI/copper joints

Figure 4 shows that the adhesion strength of PAI/copper joints decreases with increasing curing temperature of PAI. The decrease of the adhesion strength is slow up to a curing temperature of 250°C, but becomes steep at 300°C. Figure 5 shows that the FT-IR absorbance characteristic peak ratios of the amide group (1680 cm<sup>-1</sup>) and the imide group (1780 cm<sup>-1</sup>) are constant in the curing temperature interval from 200°C to 350°C when the characteristic peak of a benzene ring (1600 cm<sup>-1</sup>) is used as a standard peak. It appears that further amidation and imidization reactions did not occur with the increase of curing temperature up to 350°C, i.e. the PAI purchased from Alsthom Chemical Co. is fully amidized and imidized and its chemical structure does not change with the curing temperature from 200°C to 350°C.

The solvent content remaining in the PAI of the PAI/copper joints was measured by TGA (Fig. 6). PAI-200 had 10 wt% of solvent and PAI-250 5 wt%, but PAI-300 and PAI-350 did not have any solvent. The solvent remaining in the PAI reduces its modulus and the  $T_g$ , and increases the thermal expansion coefficient of the PAI. Therefore, as expected from equation (2), the thermal stress in PAI/copper joints



**Figure 4.** Adhesion strength of PAI/copper joints as a function of the curing temperature.



**Figure 5.** FT-IR absorbance characteristic peak ratio of amide ( $1680\text{ cm}^{-1}$ ) and imide ( $1780\text{ cm}^{-1}$ ) groups to benzene ring ( $1600\text{ cm}^{-1}$ ) of PAI as a function of the curing temperature. (●): FT-IR absorbance characteristic peak ratio of amide group ( $1680\text{ cm}^{-1}$ ) to benzene ring ( $1600\text{ cm}^{-1}$ ) of PAI. (■): FT-IR absorbance characteristic peak ratio of imide group ( $1780\text{ cm}^{-1}$ ) to benzene ring ( $1600\text{ cm}^{-1}$ ) of PAI.

is reduced with the increase of the remaining solvent in the PAI, since the effect of reducing the modulus and the  $T_g$  is larger than that of increasing the thermal expansion coefficient. Table 1 shows the variation of the Young's modulus, the  $T_g$ , the thermal expansion coefficient, and the thermal stress versus the curing temperature. The thermal stress was calculated from equation (2) and the thermal stress (residual stress – intrinsic stress) was also measured experimentally using the He–Ne laser thin film stress analyzer. As shown in Fig. 7, the thermal stress increases with increasing curing temperature, and more steeply at  $300^\circ\text{C}$ ,

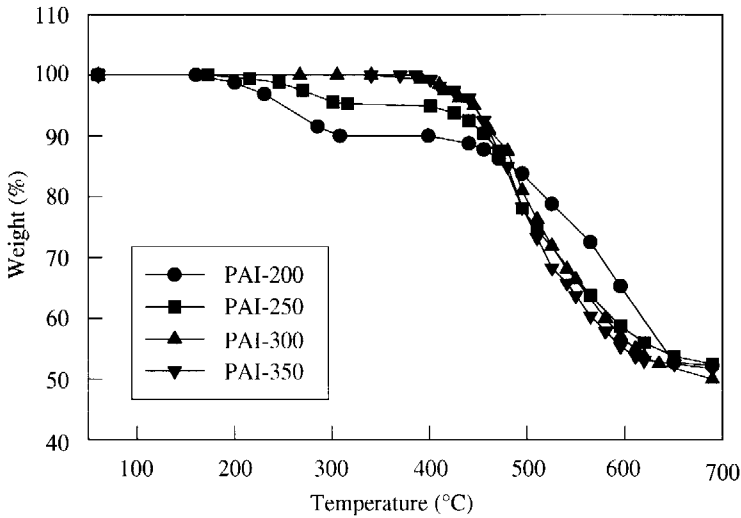


**Figure 6.** TGA diagram of cured PAI-200, PAI-250, PAI-300, and PAI-350 versus the curing temperature.

**Table 1.**

Thermal stress as a function of the curing temperature

Sample	$E$ (MPa)	$\alpha$ ( $\times 10^5$ )	$T_g$ ( $^{\circ}\text{C}$ )	$\sigma_{t,c}$ (MPa)	$\sigma_{t,e}$ (MPa)
PAI-200	1650	6.021	200.7	18.15	21.82
PAI-250	1800	5.332	230.7	19.45	22.09
PAI-300	2241	5.191	270.6	27.84	33.79
PAI-350	2506	5.044	278.4	30.77	34.20

$\sigma_{t,c}$ : thermal stress calculated by equation (2).

$\sigma_{t,e}$ : thermal stress measured experimentally by the He–Ne laser thin film stress analyzer.

which is similar to the decrease of adhesion strength (Fig. 4). This shows that the thermal stress is correlated with the adhesion strength and proportionally reduces the adhesion strength. The thermal stress measured experimentally by the He–Ne laser thin film stress analyzer is higher than the thermal stress calculated from equation (2) for all the curing temperatures. The difference between the experimental thermal stress and the calculated thermal stress originates from the experimental error in measuring the modulus, the thermal expansion coefficient, and Poisson's ratio of polyamideimide, and the thermal stress by the He–Ne laser thin film stress analysis technique. Figure 8 shows the residual stress variations with temperature for PAI-250 during curing and cooling, and then a second run of heating and cooling. The residual stress increased gradually with increasing temperature up to 150 $^{\circ}\text{C}$  and increased further during curing for 60 min at 150 $^{\circ}\text{C}$ , 200 $^{\circ}\text{C}$ , and 250 $^{\circ}\text{C}$ , since the solvent evaporated during the curing process: i.e. the residual stress increased with decreasing amount of residual solvent. After the

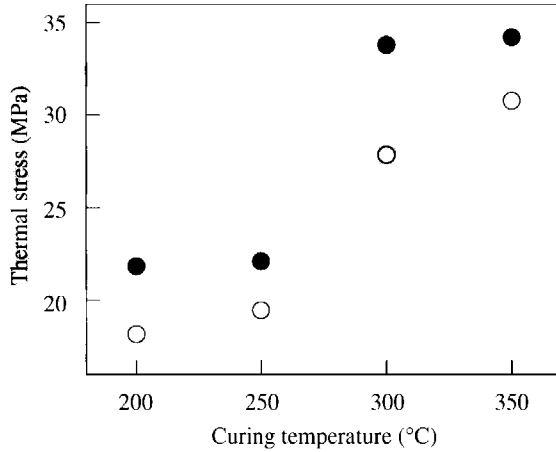


**Figure 7.** Thermal stress between PAI and copper versus the curing temperature: (○) calculated from equation (2) and (●) measured experimentally using the He–Ne laser thin film stress analyzer.

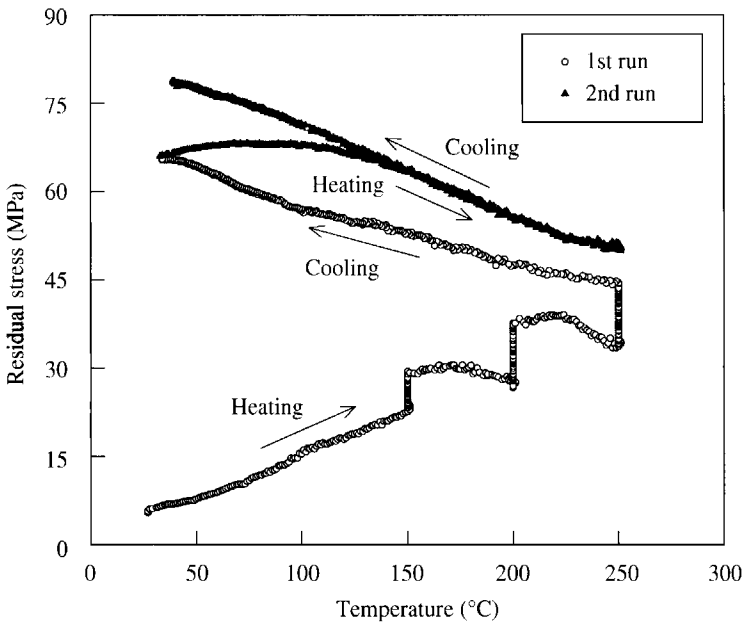


**Figure 8.** Residual stress variation with temperature in polyamideimide film measured *in situ* during heating and cooling for PAI-250: (○) 1st run, curing at 150°C for 60 min, 200°C for 60 min, and 250°C for 60 min, and cooling; (▲) 2nd run, heating and cooling. The heating rate was 2°C/min, with natural cooling.

curing was completed at 250°C for 60 min, the residual stress was 44.4 MPa and then the residual stress increased with decreasing temperature. Since the residual stress is composed of the intrinsic stress and the thermal stress, from the result of the first run of PAI-250, it appears that the intrinsic stress is 44.4 MPa and the

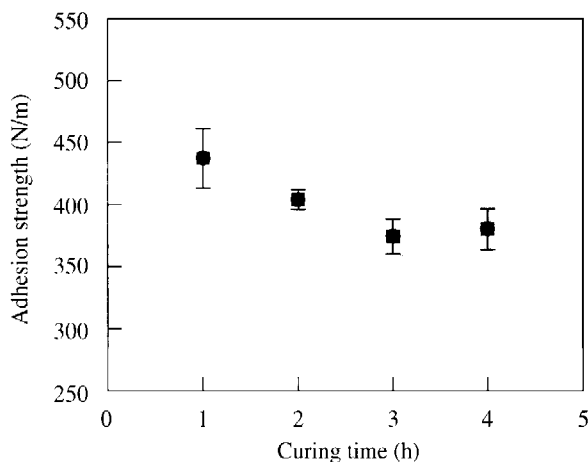


**Figure 9.** Adhesion strength of PAI-250/copper joints cured at 250 °C versus the curing time.

thermal stress is 20 MPa (first run of Fig. 8). The intrinsic stress comes generally from process-related factors such as film contamination and defects, thickness or volume reduction due to removing the solvent, and incomplete structural ordering processes [9, 21]. In order to measure the thermal stress more accurately, the above sample was heated again up to 250 °C and cooled down to room temperature (second run of Fig. 8). The residual stress increased slightly at the beginning of the heating process since the residual solvent in PAI-250 (about 5 wt% as shown in Fig. 6) evaporated during the heating process and then decreased with increasing temperature. The measured residual stress reached almost the minimum of 50.5 MPa at 230 °C and then saturated. Therefore, the intrinsic stress increased from 44.4 to 50.5 MPa as shown in the second run of Fig. 8 because of the evaporation of the solvent. Since the glass transition temperature of PAI-250 is 230.7 °C, the thermal stress became zero above the glass transition temperature. The thermal stress can be measured accurately in the cooling process of the second run from 250 °C to room temperature: i.e. the thermal stress of PAI-250 was 22.1 MPa. When we increased the curing time at 250 °C, the adhesion strength of the PAI-250/copper joints also decreased (Fig. 9). Since the remaining solvent in the PAI decreased with the increase of curing time, the modulus and the  $T_g$  increased and the thermal expansion coefficient decreased and as a result, the thermal stress increased (Table 2). This means that the decreased adhesion strength with the increase of the thermal stress originated from the decrease of the remaining solvent in PAI, which was similar to the decrease of the adhesion strength with increasing curing temperature. Table 3 shows the atomic concentrations by XPS of the peeled surfaces of PAI/copper joints cured at 200 °C. Since the copper side has a nitrogen component and the PAI side has a copper component, the locus of failure appears to be partially cohesive in both PAI and naturally formed copper oxide.

**Table 2.**

Thermal stress for PAI-250 as a function of the curing time at 250°C

Curing time (h)	$E$ (MPa)	$\alpha$ ( $\times 10^5$ )	$T_g$ ( $^{\circ}\text{C}$ )	$\sigma_{t,c}$ (MPa)
1	1800	5.332	230.20	19.45
2	1850	5.297	248.85	21.59
3	2018	5.137	258.81	23.49
4	2063	5.038	262.05	23.65

 $\sigma_{t,c}$ : thermal stress calculated by equation (2).**Table 3.**

Atomic concentrations (%) by XPS of the peeled surfaces of PAI-200/copper joints cured at 200°C

	Take-off angle (deg)	C	O	N	Cu
Copper side	30	77.9	15.7	4.6	1.8
	90	76.5	17.3	2.7	3.5
PAI side	30	78.6	13.8	7.3	0.4
	90	77.7	14.6	7.1	0.6

### 3.2. Adhesion strength of PAI/thermally oxidized copper joints

Figure 10 shows the decrease in adhesion strength of the PAI/copper joints when the copper coupons were thermally treated at 150°C or 250°C for 2 h before coating with PAI. The decrease in adhesion strength was more pronounced at 250°C. It has been reported that the adhesion strength of polymer/thermally oxidized copper joints is poor since thermally oxidized copper is nonuniform and has a low mechanical strength [13, 14].

The copper surface without thermal oxidation was very smooth and clean, but the peeled surface of the PAI/thermally oxidized copper joints was very rough and showed the particles and chunks of oxidized copper (Fig. 11).

With the increase of oxidation temperature, the particle size and the size of the chunks of oxidized copper increased, and the locus of failure was in the copper oxide layer formed by thermal oxidation as shown in Fig. 11.

### 3.3. Adhesion strength of PAI/alkali-oxidized copper joints

The adhesion strength of the PAI/copper joints increased when copper was treated with sodium chlorite and sodium hydroxide solution: the adhesion strength was 624 N/m even with 350°C curing (Fig. 12): i.e. a good adhesion strength can be maintained, although thermal stress is high with curing at 350°C. Table 4 shows the atomic concentration by XPS of the peeled surfaces of PAI/alkali-treated copper joints. The locus of failure appears to be near the interface: partially cohesive in both copper oxide and PAI, and partially interfacial. This indicates that the

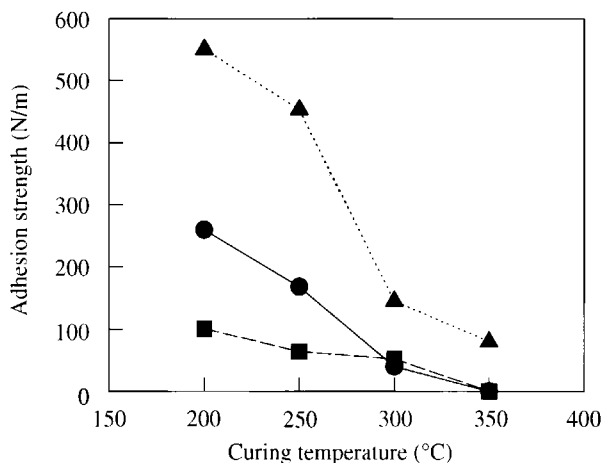


**Figure 10.** Adhesion strength of PAI/thermally treated copper joints: (▲) without thermal oxidation; (●) 150°C thermal oxidation; and (■) 250°C thermal oxidation as a function of the curing temperature.

**Table 4.**

Atomic concentrations (%) by XPS of the peeled surfaces of PAI-200/alkali-treated copper joints cured at 200°C

	Take-off angle (deg)	C	O	N	Cu
Copper side	30	58.1	30.9	1.8	9.2
	90	48.5	41.2	1.0	9.2
PAI side	30	75.6	18.6	5.2	0.5
	90	70.8	23.0	4.7	0.5

alkali-oxidized copper layer is uniform and mechanically strong compared with the thermally oxidized and naturally oxidized copper layers.

#### 4. CONCLUSIONS

The adhesion strength of the PAI/copper joints decreased with increasing curing temperature from 200°C to 350°C. The solvent content remaining in the PAI decreased as follows: 10 wt% at 200°C, 5 wt% at 250°C, and 0 wt% at 300°C. As the remaining solvent decreased, the modulus and the  $T_g$  of the PAI increased and the thermal expansion coefficient decreased. Therefore, the thermal stress increased with increasing curing temperature and reduced the adhesion strength of the PAI/copper joints. The adhesion strength also decreased with increasing curing time, since the amount of remaining solvent decreased and the thermal stress increased.

The adhesion strength of PAI/thermally oxidized copper joints was poor since the copper oxide layer formed by thermal treatment was nonuniform and mechanically

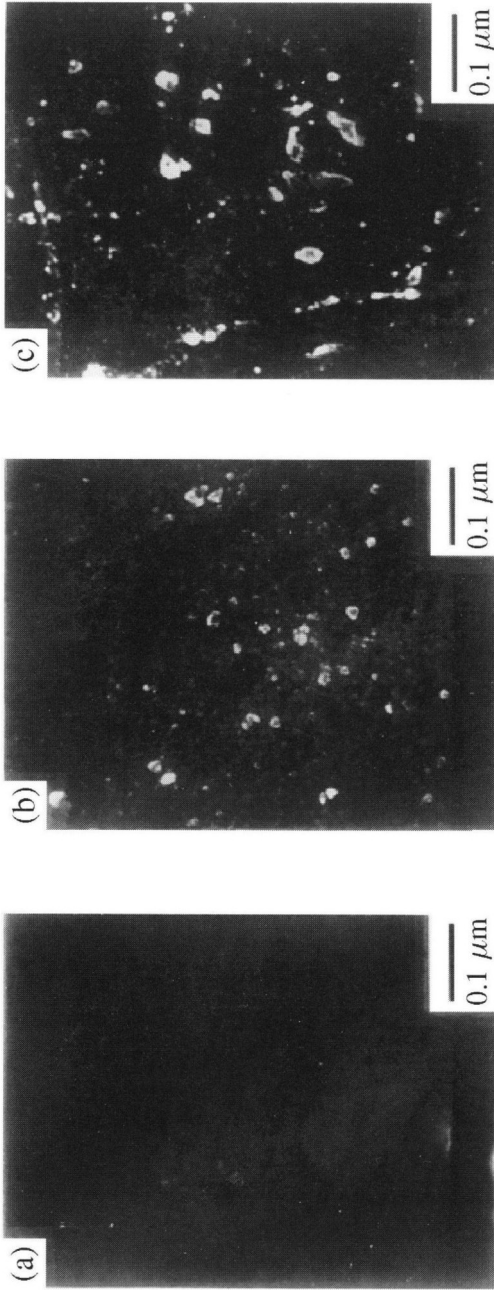


**Figure 11.** Scanning electron micrographs of the copper surface without thermal oxidation and the peeled surfaces of PAI-200/thermally oxidized copper joints: (a) copper surface without thermal oxidation; (b) peeled copper side and (c) peeled PAI-200 side of PAI-200/thermally oxidized copper at 150°C joints; and (d) peeled copper side and (e) peeled PAI-200 side of PAI-200/thermally oxidized copper at 250°C joints.

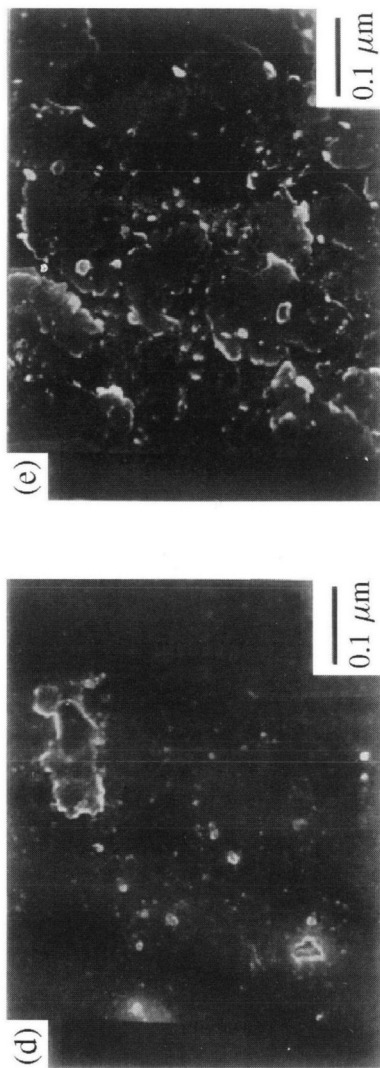
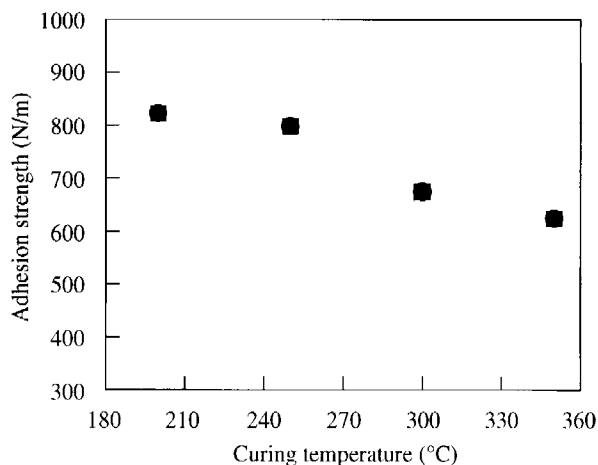


Figure 11. (Continued).



**Figure 12.** Adhesion strength of PAI/copper joints versus the curing temperature, where the copper was alkali-oxidized.

weak. A weaker copper oxide was formed at a higher thermal treatment temperature. Alkaline treatment of copper using sodium chlorite and sodium hydroxide solution increased the adhesion strength of the PAI/copper joints since very uniform and mechanically strong copper oxide was formed. In this case, a high adhesion strength (624 N/m) was maintained even at a curing temperature of 350°C.

### Acknowledgements

This work was supported by the Korea Research Institute of Chemical Technology and partially supported by the Center for Advanced Functional Polymers.

### REFERENCES

1. M. C. Burrell and J. J. Keane, *Surface Interface Anal.* **11**, 487–496 (1987).
2. H. R. Kricheldorf and M. Gurau, *J. Polym. Sci. Part A: Polym. Chem.* **33**, 2241–2250 (1995).
3. H. R. Kricheldorf and V. Linzer, *Polymer* **36**, 1893–1902 (1995).
4. J. H. Jou, C. H. Liu, J. M. Liu and J. S. King, *J. Appl. Polym. Sci.* **47**, 1219–1232 (1993).
5. K. M. Chen, S. M. Ho and T. H. Wang, *J. Appl. Polym. Sci.* **45**, 947–956 (1992).
6. S. A. Chambers and K. K. Chakravorty, *J. Vac. Sci. Technol.* **A6**, 3008–3011 (1988).
7. S. T. Chen, C. H. Yang, F. Faupel and P. S. Ho, *J. Appl. Phys.* **64**, 6690–6698 (1988).
8. M. Ree, C. W. Chu and M. J. Goldberg, *J. Appl. Phys.* **75**, 1410–1419 (1994).
9. M. Ree, T. L. Nunes, G. Czornyj and W. Volksen, *Polymer* **33**, 1228–1236 (1992).
10. M. Ree, K. J. Chen, D. P. Kirby, N. Katzenellenbogen and D. Grischkowsky, *J. Appl. Phys.* **72**, 2014–2021 (1992).
11. S. Numata, K. Fujisaki and N. Kinjo, *Polymer* **28**, 2282–2288 (1987).
12. K. L. Mittal (Ed.), *Silanes and Other Coupling Agents*. VSP, Utrecht, The Netherlands (1992).
13. L. J. Slominski and A. Landau, *Plating Surface Finish* **69**, 96–99 (1982).
14. H. K. Yun, K. Cho, J. H. An and C. E. Park, *J. Mater. Sci.* **27**, 5811–5817 (1992).
15. C. Blaauw, *J. Appl. Phys.* **54**, 5064–5068 (1983).

16. J. T. Pan and I. Blech, *J. Appl. Phys.* **55**, 2874–2880 (1984).
17. R. J. Jaccodine and W. A. Schlegel, *J. Appl. Phys.* **37**, 2429–2434 (1966).
18. F. J. von Preissig, *J. Appl. Phys.* **66**, 4262–4268 (1989).
19. S. Timoshenko, *J. Opt. Soc. Am.* **11**, 233–255 (1925).
20. U.S. Patent No. 4,409,037 (1983).
21. R. W. Hoffman, in: *Physics of Thin Film*, G. Hass and R. E. Thun (Eds), Vol. 3, pp. 219–253. Academic Press, New York (1966).